

Journal Pre-proof

An Enhanced Dual Detection of DMB-Labeled Sialic Acids Using High-Resolution Accurate Mass Spectrometry and Fluorescence Detection

Takayuki Omoto , Nao Yamakawa , Di Wu , Hitoshi Mori ,
Ushio Takeda , Masaya Hane , Ken Kitajima , Chihiro Sato

PII: S2667-1603(25)00015-8
DOI: <https://doi.org/10.1016/j.bbadv.2025.100152>
Reference: BBADVA 100152



To appear in: *BBA Advances*

Received date: 29 November 2024
Revised date: 20 February 2025
Accepted date: 28 February 2025

Please cite this article as: Takayuki Omoto , Nao Yamakawa , Di Wu , Hitoshi Mori , Ushio Takeda , Masaya Hane , Ken Kitajima , Chihiro Sato , An Enhanced Dual Detection of DMB-Labeled Sialic Acids Using High-Resolution Accurate Mass Spectrometry and Fluorescence Detection, *BBA Advances* (2025), doi: <https://doi.org/10.1016/j.bbadv.2025.100152>

This is a PDF file of an article that has undergone enhancements after acceptance, such as the addition of a cover page and metadata, and formatting for readability, but it is not yet the definitive version of record. This version will undergo additional copyediting, typesetting and review before it is published in its final form, but we are providing this version to give early visibility of the article. Please note that, during the production process, errors may be discovered which could affect the content, and all legal disclaimers that apply to the journal pertain.

© 2025 Published by Elsevier B.V.
This is an open access article under the CC BY-NC-ND license
(<http://creativecommons.org/licenses/by-nc-nd/4.0/>)

Highlights

- High-performance separation of mammalian *O*-acetylated sialic acid species with advanced fragmentation and online FLD detection.
- Identification of a set of *O*-acetylated sialic acid in bovine submaxillary mucin, including a newly identified tri-*O*-acetylated variant
- Finding of the C5-specific diagnostic fragment ions potentially distinguishing the core structure of Neu5Ac, Neu5Gc, and Kdn

Journal Pre-proof

An Enhanced Dual Detection of DMB-Labeled Sialic Acids Using High-Resolution Accurate Mass Spectrometry and Fluorescence Detection

Takayuki Omoto ^{a,#}, Nao Yamakawa ^{a,b,#}, Di Wu ^{a,c}, Hitoshi Mori ^a, Ushio Takeda ^d, Masaya Hane ^{a,c}, Ken Kitajima ^a, Chihiro Sato ^{a,c}

^a *Integrated Glyco-Biomedical Research Center (iGMED), Institute for Glyco-core Research (iGCORE), Nagoya University, Nagoya 464-8601, Japan*

^b *US 41-UAR 2014-PLBS, Université de Lille, CNRS, INSERM, CHU Lille, Institut Pasteur de Lille, Lille, France*

^c *Graduate School of Bioagricultural Sciences, Nagoya University, Nagoya 464-8601, Japan*

^d *K.K. ABSciex Japan, Shinagawa Tokyo, 140-0001, Japan*

These authors contributed equally to this work.

* Corresponding author at

Chihiro Sato, Integrated Glyco-Biomedical Research Center (iGMED), Institute for Glyco-core Research (iGCORE), Nagoya University, Nagoya 464-8601, Japan.

E-mail address: chi@agr.nagoya-u.ac.jp

Abstract

Sialic acids are important glycan components not only in the conformation of the structure but also in functions of many biological activities. Detection methods for sialic acid have been developed, and fluorescent labeling of sialic acids with 1,2-diamine-4,5-dimethylbenzene (DMB) is the best method for its analysis. However, identifying and quantifying sialic acids using mass spectrometry (MS) remains difficult because of the diversity of sialic acids, including *O*-acetylation. In this study, we initially focused on enhancing the liquid chromatography (LC) separation of DMB-labeled sialic acids in bovine submaxillary mucin (BSM). We successfully achieved highly resolute separation of 14 types of sialic acids, including multiply *O*-acetylated species, using a CAPCELL CORE C18 column. These structures were subsequently confirmed through collision-induced dissociation (CID) fragmentation. We then assessed MS and fluorescence detection (FLD) sensitivity using Neu5Ac, Neu5Gc, and Kdn standards, determining detection limits of 32 fmol for MS and 320 amol for FLD, with 320 fmol needed for CID-based structural analysis. These findings highlight the complementary nature of fluorescence and mass spectrometry techniques for DMB-labeled sialic acids identification and quantification. We also examined both CID and electron-activated dissociation (EAD) on the ZenoTOF 7600. CID fragment analysis revealed C5-specific diagnostic fragment ions for Neu5Ac, Neu5Gc, and Kdn. EAD spectra predominantly induced fragmentation of the fluorescent DMB core, regardless of applied variable kinetic energies. This study also led to the discovery of a new structure, Neu5Gc7,8,9Ac₃, alongside the previously reported Neu5,7,8,9Ac₄ in BSM.

Keywords: sialic acid, high-resolution mass spectrometry, fluorescence detection, collision-induced dissociation, electron-activated dissociation

1. Introduction

Sialic acids, a diverse family of nine-carbon monosaccharides, play crucial roles in numerous biological processes and diseases. These negatively charged sugars, which are typically found at the terminal positions of complex glycans in higher animals and some pathogenic microorganisms, exhibit remarkable structural diversity. In animals, sialic acids exist primarily in three forms: *N*-acetylneuraminic acid (Neu5Ac), *N*-glycolylneuraminic acid (Neu5Gc), and deaminoneuraminic acid (Kdn) (Fig. 1A) [1,2]. Further modifications, including phosphates, sulfates, methyl groups, lactyl groups, and additional *O*-acetyl groups, contribute to their unique biological functions [3]. The importance of sialic acids in immune system regulation and host interactions with viruses, bacterial pathogens, and microbiota has encouraged advanced analytical method development [2,4]. Chromatographic and mass spectrometric techniques have emerged as primary tools for sialic acid identification and quantification.

Gas chromatography-mass spectrometry (GC-MS) is a cornerstone of sialic acid analysis and involves separating the volatile derivatives of sialic acid methyl esters. Using heptafluorobutyrate derivatives in GC-MS analysis has historically been substantial, enabling the identification of a large number of sialic acid variants [5,6].

High-performance liquid chromatography (HPLC) methods, coupled with relatively specific fluorescent labeling reactions using benzene-diamine derivatives for α -keto acids of sialic acids, provide enhanced sensitivity for sialic acid detection [7–16]. Furthermore, DMB labeling has improved analytical capabilities, allowing detection at the femtomole level [17]. Despite these advancements, the current methods face limitations. Although fluorescent labeling offers better sensitivity than GC-MS, the low resolution of LC and collision-induced dissociation (CID) fragmentation make it challenging to observe position-specific reporter ions in structural isomers

[5]. This limitation hinders detailed substituent position identification without authentic samples. In this study, we explored the advanced use of fragmentation in DMB-Sia analysis with the aim of discovering a potential tool for identifying the detailed structural characteristics of various sialic acids. We employed high-resolution, high-accuracy mass spectrometry (HRMS) with CID to generate diagnostic product ions specific to sialic acid species, providing structural information that was not previously reported using conventional CID spectra. Additionally, we investigated an electron-activated dissociation (EAD) fragmentation on DMB-Sia to understand its capabilities in sialic acid analysis. The ZenoTOF 7600, the latest generation of quadrupole time-of-flight (Q-TOF) instruments, has introduced a novel radio-frequency ion trap to achieve fast electron-based dissociation. The novel radio-frequency ion trap enables versatile electron activated dissociation (EAD), supporting both electron capture dissociation (ECD) for multiply protonated peptides and proteins, and electron impact excitation of ions from organics (EIEIO) for efficient fragmentation of singly charged ions using high-energy free electrons [18–20]. This study presents an advanced analytical approach that combines the efficient separation of DMB-labeled sialic acids on a reversed-phase column with electrospray ionization (ESI) integrated with HRMS. Our method employs scheduled high-resolution multiple reaction monitoring (sMRM^{HR}) in HRMS for quantitative analysis, offering improved quantitative efficiency through high-speed scanning and providing critical information on the sialic acid structure via indicator ions obtained using CID.

While the early use of EAD revealed some limitations, ongoing improvements in this technique are expected to further advance the ability to elucidate complex sialic acid structures, resolve their structural isomers, and determine substituent positions in sialic acid variants.

We have developed an improved workflow for sialic acid analysis that combines high-resolution column separation, fluorescence detection, and HRMS-CID. This approach enhances the qualitative analysis of structural characteristics and increases the reliability of structural identification in sialic acid analysis.

2. Results and Discussion

2.1. Analysis of BSM and standard sialic acid using fluorescence detection, information-dependent acquisition (IDA), and sMRM^{HR}

Fluorescent-labeled sialic acid analysis has been developed and used since the 1980s as a method for identifying and quantifying sialic acid molecular species because of its high sensitivity. However, while the relatively low resolution of LC and the instability of labeled sialic acids remain to be addressed, other diamine derivatives, such as *o*-phenylenediamine (OPD) [8] and 4,5-dimethylbenzene-1,2-diamine (DMBA) [10,21], have also been studied as candidates for improving LC performance, in addition to the conventional method, DMB-Sia (Fig. 1B). Here, we investigated the optimal conditions for detecting DMB-Sia by combining LC separation and fluorescence detection with online mass spectroscopy (MS) and tandem mass spectroscopy (MS/MS) analysis using the latest high-resolution accurate mass spectrometry ZenoTOF 7600 Q-TOF system from Sciex.

First, we examined the LC separation of DMB derivatives using BSM, Neu5Ac, Neu5Gc, Kdn, Neu5,9Ac₂, and Neu4,5Ac₂ as reference standards (Fig. S1 and S2), and evaluated the results using fluorescence detection and MS. We had previously encountered problems with the separation of Neu5Gc7Ac and Neu5Ac; however, here we demonstrated that separating all 14

peaks containing Neu5Ac and Neu5Gc with multiple *O*-acetyl substituents is possible using a CAPCELL CORE C18 column (Fig. 2). Regarding structures with two *O*-acetyl groups, the elution position of the peak is predictable based on changes in sialic acid hydrophobicity due to the position of the acetyl groups [21]. In this study, we observed that a compound with an *O*-acetyl group at position 4 was eluted before acetylation at C9 on the CAPCELL CORE C18 column, despite C9 acetylation being accounted for by its lower hydrophobicity [21]. This unexpected elution order suggests that factors beyond hydrophobicity, such as steric hindrance, must be considered when interpreting the chromatographic behavior of the column used in this study. Consequently, we have not attributed specific positions to these groups and have instead denoted them with " χ ". The extracted ion chromatograms (XICs) revealed peaks at m/z 552.182 and m/z 568.177, corresponding to Neu5Ac and Neu5Gc, respectively, each with three *O*-acetyl groups. This study identified the presence of DMB-Neu5Gc with three *O*-acetyl groups in BSM in addition to the previously reported DMB-Neu5Ac. These structures were initially detected using fluorescence and subsequently confirmed using CID fragmentation analysis (Fig. 2 and S3). Based on previous findings and analysis of the standard sample used in this study (Fig. 3, S1, and S2), it was evident that structures with an acetyl group at position 4 exhibited negligible $[M-18+H]^+$ fragmentation. Consequently, we propose that the Neu5, $\chi\chi\chi$ Ac₄ and Neu5Gc $\chi\chi\chi$ Ac₃ detected in this study are likely Neu5,7,8,9Ac₄ and Neu5Gc7,8,9Ac₃, respectively. Using 5 ng of BSM, we identified the structures of 14 types of sialic acids using CID fragmentation and compared the relative abundances of each sialic acid species (Fig. 2, 4, S3, and Table 1). Despite the low signal-to-noise (S/N) ratio for peak 14, Neu5Gc7,8,9Ac₃, at 5 ng of BSM, we confirmed its presence based on two key factors. First, its retention time at 60.99 min matched that observed with 50 ng of BSM. Second, we detected a set of fragment ions at peak 14 that

perfectly aligned with the fragment profile observed at 50 ng of BSM (Fig. S4). These consistent characteristics allowed us to confidently identify the structure even at the lower concentration. In this study, we employed IDA analysis in positive ion mode to identify DMB-Sia species in BSM. Based on previous reports of lactyl group presence on Neu5Ac in BSM [22], we investigated the occurrence of this modification, as well as potential methyl groups and DMB-Kdn, which could be detectable under the same conditions. Our findings revealed no evidence of DMB-Kdn or methylated Sia. However, we observed slight indications of lactyl modification, consistent with previous reports. To conclusively confirm the fragmentation pattern of lactyl-modified Sia, further MS/MS analysis will be necessary. This approach provides the basis for a more comprehensive characterization of Sia modifications in BSM.

Next, the quantitative performance and detection sensitivity of time-of-flight mass spectrometry (TOF-MS) was examined. DMB-labeled sialic acids exhibit strong fluorescence, making them widely utilized for the detection of trace amounts of sialic acid with high sensitivity. However, for DMB-labeled sialic acids that lack a standard product, evaluating their characteristics solely through fluorescence detection is challenging. Additionally, identifying components that cannot be separated using HPLC becomes impossible. Therefore, employing mass spectrometry allows for the reduction of interference caused by co-elution and enables the identification and quantification of individual components.

In this study, we utilized sMRM^{HR} to measure quantitative performance in specific DMB-Sia compounds (Fig. 5). The results indicated that while 32 fmol of DMB-Neu5Ac was necessary for sMRM^{HR} analysis, the detection limit for fluorescence detection was established at 320 amol with higher quantitative performance. Furthermore, a minimum of 320 fmol was required for

structural determination using CID fragmentation. The same results were observed for DMB-Neu5Gc and DMB-Kdn in terms of detection sensitivity (data not shown).

2.2. CID fragmentation

We analyzed the fragmentation patterns of CID to evaluate the feasibility of characterizing and determining the structures of the DMB-labeled sialic acid species. For the MS/MS CID fragments, the CAD energy intensity was investigated by varying it between CAD25 and 50. As a result, we adopted CAD30, which is an energy value expected to produce sufficient fragment effects and simultaneously and reliably produce molecular ions $[M+H]^+$, and obtained all CID spectra for comparison and evaluation. The fragmentation of DMB-Sias produces a series of specific fragment ions that retain the DMB backbone, which we term the "characteristic ion set" in this study (Tables 1 and 2). This set includes, but is not limited to, m/z values: 331.093, 313.082, 301.082, 295.072, 283.071, 271.071, 259.071, 241.061, 229.061, and 217.061. Some of these ions have been previously documented [9,12]. Importantly, each DMB-Sia forms a distinctive fragmentation pattern with characteristic peak intensity proportions under given CID parameter conditions. Both animal-type sialic acids and bacterial nonulosonic acids (NulOs) exhibit distinct yet related CID fragmentation patterns [9,12,13]. These universal fragmentation patterns serve as a foundation for structural characterization and differentiation within the sialic acid family. The identification of DMB-derivatized sialic acids (DMB-Sia) has traditionally relied on a combination of retention time and MS, MS², or MS³ fragmentation patterns. Here, we further focused on specific fragments that serve as clues to identify certain chemical structures or specific group about the sialic acid moieties. We investigated these fragments' potential as indicators for structural identification and termed them "Diagnostic ions". We successfully

identified a group of fragments arising from differences in the modifications at the C5 position (Table 2). Although the generation process of some fragments remains only partially understood, we clarified the ion structures using high mass accuracy, ranging from several parts per million (ppm) to 10 ppm, and proposed several possible fragment structures (Table 2). HRAM mass spectrometry offers precise mass measurements and detailed product ion spectra, crucial for component identification and verification. It enables accurate determination of elemental compositions through precise m/z values, providing detailed molecular structure information. This precision is particularly valuable for analyzing complex mixtures, helping to resolve isobaric interference and enhancing analyte detection. The CID spectrum revealed multiple prominent fragments arising from differences in the C5 substituent (Table 2). For instance, the fragments at m/z 126.055, 138.055, and 168.066 corresponded to the *N*-acetyl group at the C5 position, which is unique to Neu5Ac. The proposed ion molecular formula and fragment ion structure are shown in Table 2. The fragment ion at m/z 168.066 was notably prominent Neu5Ac species carrying *O*-acetyl group modifications. Notably, *O*-acetylation specifically at the C4 position did not influence the intensity of this fragment (Fig. 3, 4, S2, and S3). Furthermore, ions reflecting the differences at the C5 position were observed at m/z 142.050, 154.050, and 184.060 for Neu5Gc and m/z 127.039 and 129.054 for Kdn. Notably, for Neu5Gc, the fragment ion at m/z 184.060 increased substantially owing to *O*-acetyl group modification, similar to the behavior observed for Neu5Ac (Fig. 4). These variations in the fragment patterns clearly highlight the structural differences among sialic acid species and provide crucial insights for their identification and structural analysis. Tables 1 and 2 present a compilation of prominent ion sets observed in our analysis, which we refer to as "characteristic ion set". These sets are listed in an order of decreasing intensity, focusing on the m/z range of 80 to 380. The CID spectra of minor

components in BSM (peaks 6, 7, and 12–14) exhibited low S/N ratios (Fig. 2, 4, and S3) and occasionally displayed notable non-identifiable background peaks not attributed to DMB-Sia. The HRAM data enabled precise molecular formula determination for each ion, effectively filtering out ambiguous components and allowing focused analysis of the relevant product ion spectra. We observed that in low S/N ratio spectral data, the mass accuracy for some detected peaks decreased to 60–80 ppm. However, the detection of ions resulting from a loss of water molecules and substituents from the molecular ions provides additional support for the identification of the characteristic ion set. This complementary information helps to validate the presence of specific sialic acid structures, even when mass accuracy is compromised due to low signal intensity. In this study, we explored novel EAD technology on ZenoTOF 7600 with CID to compare the fragmentation characteristics relevant to the structural analysis of sialic acids (Fig. 6).

2.3. EAD fragmentation

Although electron-based ion fragmentation techniques (ExD) are not commonly used for structural analysis of oligosaccharides, previous studies have demonstrated the effectiveness of electron-transfer dissociation (ETD) fragmentation for milk oligosaccharides and electron-capture dissociation (ECD) fragmentation using alkali and alkaline earth metals. These findings suggest that these methods can serve as valuable alternatives to supplement CID fragmentation information [23–25]. Additionally, EAD analysis has been reported for *N*-acetylglucosamine, demonstrating its effectiveness in providing extensive fragment and structural information compared to CID [26]. In this study, EAD analysis was conducted on DMB-Sias for the first time. The analysis was performed by comparing the kinetic energies (KE) of 8, 12, 16, and 20 eV. Among the energies compared, no significant difference was observed in the fragmentation

patterns. However, at 20 eV, while the number of intermediate-sized fragments decreased, the number of smaller fragments increased. In this study, the spectrum obtained at the KE of 16 eV was compared to the CID spectrum (Fig. 6).

Analysis of the EAD spectra of DMB-Sias revealed that both radical and non-radical ion fragmentation processes occur around the DMB core. This is significant because DMB, a fluorescent molecule, acts as an effective electron acceptor and influences the fragmentation patterns observed in the EAD spectrum. Specifically, we identified prominent fragments in the EAD spectra that were dependent on the DMB core structure, indicating that these fragments originated from the DMB structure itself. Similarly, the benzyl (m/z 91.054) and radical benzyl (m/z 92.062) ions, which are thought to be derived from the DMB structure, were observed in the EAD spectrum. These findings highlight the role of the DMB core as a structural component that facilitates specific fragmentation pathways. Our investigation into the effects of varying kinetic energies on DMB-Sias fragmentation yielded no significant improvements in structural information. Consequently, we have shifted our focus to exploring alternative fragmentation enhancement strategies. Inspired by previous EXD studies on oligosaccharides [23–25], we are evaluating the potential of alkali metals to promote efficient inner-cleavage processes within the sugar moiety. We aim to adapt these promising approaches to enhance fragmentation patterns for both DMB-labeled and non-labeled Sia analysis using EAD analysis, potentially yielding deep structural insights in future studies.

3. Conclusions

We investigated the potential of detecting and quantitatively analyzing DMB-labeled sialic acids using a recently developed ZenoTOF 7600 Q-TOF mass spectrometer. We successfully separated

14 types of sialic acid molecules under the optimized conditions for the high-resolution CAPCELL CORE C18 analytical column employed in our analysis. Using BSM, we identified the structures of all the sialic acids using CID spectra with a sample size of only 5 ng. Furthermore, we explored the potential of quantitative analysis using Q-TOF MS and compared it with traditional fluorescence detection methods. Our results demonstrate that quantitative analysis via high-speed scanning is achievable with a sensitivity threshold of 32 fmol using the sMRM^{HR} method.

Integrating a fluorescence detector coupled with a mass spectrometer facilitated the efficient exclusion of peaks associated with the DMB degradation byproducts. This setup allowed for simultaneous analysis of the data obtained from both fluorescence detection and MS, ensuring a consistent analytical approach.

Additionally, this study marks the first analysis of DMB-sialic acid using EAD, compared to CID fragmentation. We characterized the EAD fragmentation spectrum of DMB-sialic acid and highlighted significant differences in the fragmentation patterns, particularly regarding the fluorescent DMB moiety. This comparison revealed critical issues that must be addressed in future studies to facilitate fragmentation, specifically of the sialic acid moiety.

Both the CID and EAD spectra benefited from high-accuracy mass analysis, enabling the precise measurement of structural fragment ions with an error margin ranging from a few ppm to 10 ppm. This accuracy allowed us to effectively predict the fragment structures of DMB-modified sialic acids. Consequently, we present several previously uncharacterized fragment ion structures of DMB-modified sialic acids, including multiple ions generated from the sialic acid moieties which provides the structural characteristics of sialic acid group, particularly differentiating C5 position modifications. By analyzing the patterns of the generated fragment

ions, we obtained detailed information regarding the structure and modification of the sialic acids. We anticipate that advancements in this analytical technology will contribute to the elucidation of new structures within sialic acid molecular species.

4. Materials and Methods

4.1. Materials

Neu5Ac and trifluoroacetic acid (TFA) were purchased from NACALAI TESQUE (Kyoto, Japan). Sodium hydrosulfite, 2-mercaptoethanol, and propionic acid were purchased from FUJIFILM Wako (Osaka, Japan). Neu5Gc was purchased from the Tokyo Chemical Industry (Tokyo, Japan). Neu5,9Ac₂ was isolated from lake trout polysialoglycoproteins (PSGP) [1]. Neu4,5Ac₂ has been isolated from freshwater trout hyosophorin [27]. Furthermore, DMB was purchased from Dojindo (Kumamoto, Japan). Methanol, acetonitrile, and 0.1% (v/v) formic acid in water were purchased from KANTO CHEMICAL (Tokyo, Japan). BSM was purchased from MP Biomedicals (Irvine, CA, USA).

4.2. Derivatization of sialic acids with DMB

Sialic acids in 2 µg of BSM or 1 µg of standard samples were released through mild acid hydrolysis in 2 M propionic acid at 80°C for 2 h, and the hydrolysates were dried immediately under vacuum. The dried samples were dissolved in 20 µL of 0.01 N TFA and 20 µL of 7 mM DMB solution in 5 mM TFA containing 1 M 2-mercaptoethanol and 18 mM sodium hydrosulfite and incubated at 50°C for 2 h in dark conditions. Based on previous reports [28–30], the conditions for acid hydrolysis while maintaining the *O*-acetyl group on the sialic acid were investigated using a combination of acetic acid, propionic acid, and TFA, and the optimal

hydrolysis time was also re-examined. The current conditions were confirmed to be optimal and adopted.

4.3. Analysis of sialic acids using LC-MS

The DMB-derivatized sialic acids were analyzed using an LC-MS system consisting of a Shimadzu Nexera system (Shimadzu, Kyoto, Japan) and a ZenoTOF 7600 mass spectrometer (Sciex, Framingham, MA, USA). The Nexera system controller (SCL-40) was equipped with a pump unit (LC-40D), a degasser (DGU-405), and an auto-sampler (SIL-40C). Chromatographic separation of the DMB-derivatized sialic acids was performed using a CAPCELL CORE C18 column (2.7 μm , 2.1 mm i.d. \times 150 mm, OSAKA SODA, Japan) maintained at 30°C by column oven (CTO-40S). The mobile phase consisted of 0.1% (v/v) formic acid in water (A) and acetonitrile : methanol (50:50, v/v) (B). The flow rate was set at 0.2 mL/min, and 5 ng of BSM or 1 ng of the standard sample was injected for each run. The gradient was set as follows: 8% B (0–24.0 min), 8–30% B (24.0–80.0 min), 30–95% B (80.0–80.1 min), 95% B (80.1–85.0 min), 95–8% (85.0–85.1 min), 8% B (85.1–90.0 min), with a total run time of 90 min. Fluorescence detection was performed using an RF-20A XS fluorescence detector with excitation (Ex) and emission (Em) wavelengths set at 373 and 448 nm, respectively.

MS analysis was conducted using the ZenoTOF 7600 system, with MS/MS spectra acquired by information-dependent acquisition (IDA) and sMRM^{HR} methods. Two dissociation methods, EAD and CID, were employed for fragment ion analysis. The MS was initially set to MS (TOF-MS) and MS/MS (IDA) modes, followed by sMRM^{HR} mode for quantitative analysis, considering the retention time of each target component obtained by the IDA method. The instrument was operated in positive ion mode with the following parameters: curtain gas, 40 psi;

ion source gas 1, 60 psi; ion source gas 2, 60 psi; CAD gas, 7; source temperature, 300°C; ion spray voltage, 5,500 V. The TOF-MS and TOF-MS/MS ranges were set to 100–1,000 Da and 80–1,000 Da, respectively. The accumulation time was set to 0.10 s for TOF-MS, 0.25 s for CID, and 0.50 s for EAD. The EAD and CID parameters were set as follows: For EAD, the electron beam current was 7,000 nA with the electron KE values of 16 eV and a CE value of 10 V. The reaction time was set to 45 s. For CID, the CE value was 30 V with a reaction time of 30 s. Data analysis was performed using the SCIEX OS software (version 3.4, SCIEX, Framingham, MA, USA).

4.4. Analysis of detection limits of fluorescence and XIC in standard Neu5Ac

A serial 10-fold dilution of standard Neu5Ac in Milli-Q water was carried out to prepare sample amounts in the range of 3.2 pmol to 3.2 amol, which were then derivatized with DMB. The samples were subjected to LC-MS analysis, and the calibration curves for each sample were plotted using fluorescence detection (Ex/Em: 373/448 nm), sMRM^{HR} for CAD30 and EAD16, respectively. The LC-MS conditions were performed as described above, and the gradient conditions were as follows: 8% B (0–24.0 min), 8–30% B (24.0–30.0 min), 30–95% B (30.0–30.1 min), 95% B (30.1–35.0 min), 95–8% (35.0–35.1 min), 8% B (35.1–40.0 min) for a total run time of 40 min.

5. CRediT authorship contribution statement

Conceptualization, T.O., N.Y., C.S.: Data curation, T.O., N.Y., D.W., C.S.: Formal analysis, N.Y., C.S.: Funding acquisition, D.W., H.M.C.S. : Investigation, T.O., N.Y., D.W., H.M., C.S. : Methodology, T.O., N.Y., D.W., C.S. : Project administration, T.O., K.K., C.S. : Resources, T.O., C.S.: Software, D.W., C.S.: Supervision, C.S. : Validation, T.O., N.Y., U.T., M.H., C.S. :

Visualization, T.O., N.Y., D.W., K.K., C.S.: Writing – original draft, T.O., N.Y., C.S.: Writing – review & editing, T.O.,N.Y.,D.W.,U.T.,M.H.,K.K.,C.S.

6. Declaration of competing interest

The authors declare that they have no known competing financial interests or personal relationships that could have appeared to influence the work reported in this paper.

7. Acknowledgments

This research was funded by the Japan Agency for Medical Research and Development (AMED) [grant number 23gm6410007h0004] (to CS) and a Grant-in-Aid for Scientific Research(B) (21H02425 and 23K21291) from JSPS (to CS). A part of this work is supported by J-Glyconet (JGN) and human glycome atlas project (HGA). This work was also supported by Novartis Research Grants from The Novartis Foundation (to DW) and grant-in-Aid for Scientific Research C (24K08829) to MH. We would like to express our gratitude to the plateforme d'analyses des glycoconjugués (PAGés) platform for facilitating the exchange of knowledge and expertise, as well as for fostering valuable discussions.

8. References

- [1] C. Sato, K. Kitajima, I. Tazawa, Y. Inoue, S. Inoue, F.A. Troy, Structural diversity in the alpha 2→8-linked polysialic acid chains in salmonid fish egg glycoproteins. Occurrence of poly(Neu5Ac), poly(Neu5Gc), poly(Neu5Ac, Neu5Gc), poly(KDN), and their partially acetylated forms., *Journal of Biological Chemistry* 268 (1993) 23675–23684. [https://doi.org/10.1016/S0021-9258\(19\)49515-X](https://doi.org/10.1016/S0021-9258(19)49515-X).
- [2] K. Kitajima, N. Varki, C. Sato, Advanced Technologies in Sialic Acid and Sialoglycoconjugate Analysis, in: R. Gerardy-Schahn, P. Delannoy, M. Von Itzstein (Eds.), *SialoGlyco Chemistry and Biology II*, Springer International Publishing, Cham, 2013: pp. 75–103. https://doi.org/10.1007/128_2013_458.

- [3] C.L. Wardzala, A.M. Wood, D.M. Belnap, J.R. Kramer, Mucins Inhibit Coronavirus Infection in a Glycan-Dependent Manner, *ACS Cent. Sci.* 8 (2022) 351–360. <https://doi.org/10.1021/acscentsci.1c01369>.
- [4] A. Mori, M. Hane, Y. Niimi, K. Kitajima, C. Sato, Different properties of polysialic acids synthesized by the polysialyltransferases ST8SIA2 and ST8SIA4, *Glycobiology* 27 (2017) 834–846. <https://doi.org/10.1093/glycob/cwx057>.
- [5] A. Pons, C. Richet, C. Robbe, A. Herrmann, P. Timmerman, G. Huet, Y. Leroy, I. Carlstedt, C. Capon, J.-P. Zanetta, Sequential GC/MS Analysis of Sialic Acids, Monosaccharides, and Amino Acids of Glycoproteins on a Single Sample as Heptafluorobutyrate Derivatives, *Biochemistry* 42 (2003) 8342–8353. <https://doi.org/10.1021/bi034250e>.
- [6] J.-P. Zanetta, A. Pons, M. Iwersen, C. Mariller, Y. Leroy, P. Timmerman, R. Schauer, Diversity of sialic acids revealed using gas chromatography/mass spectrometry of heptafluorobutyrate derivatives, *Glycobiology* 11 (2001) 663–676. <https://doi.org/10.1093/glycob/11.8.663>.
- [7] S. Hara, Y. Takemori, M. Yamaguchi, M. Nakamura, Y. Ohkura, Fluorometric high-performance liquid chromatography of N-acetyl- and N-glycolylneuraminic acids and its application to their microdetermination in human and animal sera, glycoproteins, and glycolipids, *Analytical Biochemistry* 164 (1987) 138–145. [https://doi.org/10.1016/0003-2697\(87\)90377-0](https://doi.org/10.1016/0003-2697(87)90377-0).
- [8] K.R. Anumula, Rapid Quantitative Determination of Sialic Acids in Glycoproteins by High-Performance Liquid Chromatography with a Sensitive Fluorescence Detection, *Analytical Biochemistry* 230 (1995) 24–30. <https://doi.org/10.1006/abio.1995.1432>.
- [9] A. Klein, S. Diaz, I. Ferreira, G. Lamblin, P. Roussel, A.E. Manzi, New sialic acids from biological sources identified by a comprehensive and sensitive approach: liquid chromatography-electrospray ionization-mass spectrometry (LC-ESI-MS) of SIA quinoxalinones, *Glycobiology* 7 (1997) 421–432. <https://doi.org/10.1093/glycob/7.3.421>.
- [10] L. Wang, D. Wang, X. Zhou, L. Wu, X.-L. Sun, Systematic investigation of quinoxaline derivatization of sialic acids and their quantitation applicability using high performance liquid chromatography, *RSC Adv.* 4 (2014) 45797–45803. <https://doi.org/10.1039/C4RA08930H>.
- [11] F. Wang, B. Xie, B. Wang, F.A. Troy, LC–MS/MS glycomic analyses of free and conjugated forms of the sialic acids, Neu5Ac, Neu5Gc and KDN in human throat cancers, *Glycobiology* 25 (2015) 1362–1374. <https://doi.org/10.1093/glycob/cwv051>.
- [12] H.B.C. Kleikamp, Y.M. Lin, D.G.G. McMillan, J.S. Geelhoed, S.N.H. Naus-Wiezer, P. Van Baarlen, C. Saha, R. Louwen, D.Y. Sorokin, M.C.M. Van Loosdrecht, M. Pabst, Tackling the chemical diversity of microbial nonulosonic acids – a universal large-scale survey approach, *Chem. Sci.* 11 (2020) 3074–3080. <https://doi.org/10.1039/C9SC06406K>.
- [13] T. Dubois, F. Krzewinski, N. Yamakawa, C. Lemy, A. Hamiot, L. Brunet, A.-S. Lacoste, Y. Knirel, Y. Guerardel, C. Faille, The *sps* Genes Encode an Original Legionaminic Acid Pathway Required for Crust Assembly in *Bacillus subtilis*, *mBio* 11 (2020) e01153-20. <https://doi.org/10.1128/mBio.01153-20>.
- [14] J. Ricaldi N, M.A. Matthias, J.M. Vinetz, A.L. Lewis, Expression of sialic acids and other nonulosonic acids in *Leptospira*, *BMC Microbiol* 12 (2012) 161. <https://doi.org/10.1186/1471-2180-12-161>.

- [15] N. Yamakawa, J. Vanbeselaere, L.-Y. Chang, S.-Y. Yu, L. Ducrocq, A. Harduin-Lepers, J. Kurata, K.F. Aoki-Kinoshita, C. Sato, K.-H. Khoo, K. Kitajima, Y. Guerardel, Systems Glycomics of Adult Zebrafish Identifies Organ-Specific Sialylation and Glycosylation Patterns, *Nat Commun* 9 (2018) 4647. <https://doi.org/10.1038/s41467-018-06950-3>.
- [16] A.L. Lewis, N. Desa, E.E. Hansen, Y.A. Knirel, J.I. Gordon, P. Gagneux, V. Nizet, A. Varki, S.-I. Hakomori, Innovations in Host and Microbial Sialic Acid Biosynthesis Revealed by Phylogenomic Prediction of Nonulosonic Acid Structure, *Proceedings of the National Academy of Sciences of the United States of America* 106 (2009) 13552–13557.
- [17] C. Sato, S. Inoue, T. Matsuda, K. Kitajima, Development of a highly sensitive chemical method for detecting alpha2-->8-linked oligo/polysialic acid residues in glycoproteins blotted on the membrane, *Anal Biochem*, 262, 191-197. [https://doi: 10.1006/abio.1998.2718](https://doi.org/10.1006/abio.1998.2718).
- [18] R.B. Cody, B.S. Freiser, Electron impact excitation of ions in Fourier transform mass spectrometry, *Anal. Chem.* 59 (1987) 1054–1056. <https://doi.org/10.1021/ac00134a026>.
- [19] T. Baba, J.L. Campbell, J.C.Y. Le Blanc, J.W. Hager, B.A. Thomson, Electron Capture Dissociation in a Branched Radio-Frequency Ion Trap, *Anal. Chem.* 87 (2015) 785–792. <https://doi.org/10.1021/ac503773y>.
- [20] T. Baba, J.L. Campbell, J.C.Y. Le Blanc, P.R.S. Baker, J.W. Hager, B.A. Thomson, Development of a Branched Radio-Frequency Ion Trap for Electron Based Dissociation and Related Applications, *Mass Spectrom (Tokyo)* 6 (2017) A0058. <https://doi.org/10.5702/massspectrometry.A0058>.
- [21] J. Du, Q. Zhang, J. Li, Q. Zheng, LC-MS in combination with DMBA derivatization for sialic acid speciation and distribution analysis in fish tissues, *Anal. Methods* 12 (2020) 2221–2227. <https://doi.org/10.1039/D0AY00100G>.
- [22] R. Schauer, J. Haverkamp, M. Wember, J.F.G. Vliegthart, J.P. Kamerling, *N*-Acetyl-9-*O*-*L*-lactylneuraminic Acid, a New Acylneuraminic Acid from Bovine Submandibular Gland, *European Journal of Biochemistry* 62 (1976) 237–242. <https://doi.org/10.1111/j.1432-1033.1976.tb10153.x>.
- [23] L. Han, C.E. Costello, Electron Transfer Dissociation of Milk Oligosaccharides, *J. Am. Soc. Mass Spectrom.* 22 (2011) 997–1013. <https://doi.org/10.1007/s13361-011-0117-9>.
- [24] J.T. Adamson, K. Håkansson, Electron Capture Dissociation of Oligosaccharides Ionized with Alkali, Alkaline Earth, and Transition Metals, *Anal. Chem.* 79 (2007) 2901–2910. <https://doi.org/10.1021/ac0621423>.
- [25] Y. Huang, Y. Pu, X. Yu, C.E. Costello, C. Lin, Mechanistic Study on Electron Capture Dissociation of the Oligosaccharide-Mg²⁺ Complex, *J. Am. Soc. Mass Spectrom.* 25 (2014) 1451–1460. <https://doi.org/10.1007/s13361-014-0921-0>.
- [26] J.J. Wolff, L. Chi, R.J. Linhardt, I.J. Amster, Distinguishing Glucuronic from Iduronic Acid in Glycosaminoglycan Tetrasaccharides by Using Electron Detachment Dissociation, *Anal. Chem.* 79 (2007) 2015–2022. <https://doi.org/10.1021/ac061636x>.
- [27] K. Ishii, M. Iwasaki, S. Inoue, P.T.M. Kenny, H. Komura, Y. Inoue, Free Sialooligosaccharides Found in the Unfertilized Eggs of a Freshwater Trout, *Plecoglossus altivelis*, *Journal of Biological Chemistry* 264 (1989) 1623–1630. [https://doi.org/10.1016/S0021-9258\(18\)94232-8](https://doi.org/10.1016/S0021-9258(18)94232-8).

- [28] A. Klein, M. Krishna, N.M. Varki, A. Varki, 9-O-acetylated sialic acids have widespread but selective expression: analysis using a chimeric dual-function probe derived from influenza C hemagglutinin-esterase, *PNAS* 91 (1994) 7782–7786.
<https://doi.org/10.1073/pnas.91.16.7782>.
- [29] T.P. Mawhinney, D.L. Chance, Hydrolysis of Sialic Acids and O-Acetylated Sialic Acids with Propionic Acid, *Analytical Biochemistry* 223 (1994) 164–167.
<https://doi.org/10.1006/abio.1994.1564>.
- [30] S. Hara, M. Yamaguchi, Y. Takemori, K. Furuhashi, H. Ogura, M. Nakamura, Determination of mono-O-acetylated N-acetylneuraminic acids in human and rat sera by fluorometric high-performance liquid chromatography, *Analytical Biochemistry* 179 (1989) 162–166.
[https://doi.org/10.1016/0003-2697\(89\)90218-2](https://doi.org/10.1016/0003-2697(89)90218-2).

9. Footnotes

CID	collision-induced dissociation
EAD	electron-activated dissociation
Kdn	deaminoneuraminic acid
DMB	1,2-diamine-4,5-dimethylbenzene
HPLC	high-performance liquid chromatography
MS	mass spectrometry
HRAM	high-resolution, accurate-mass
HRMS	high-resolution and high-accuracy mass spectrometer
sMRM ^{HR}	scheduled high-resolution multiple reaction monitoring
Neu5Ac	<i>N</i> -acetylneuraminic acid
Neu5Gc	<i>N</i> -glycolylneuraminic acid

Figure legends

Fig. 1 (Omoto et al.)

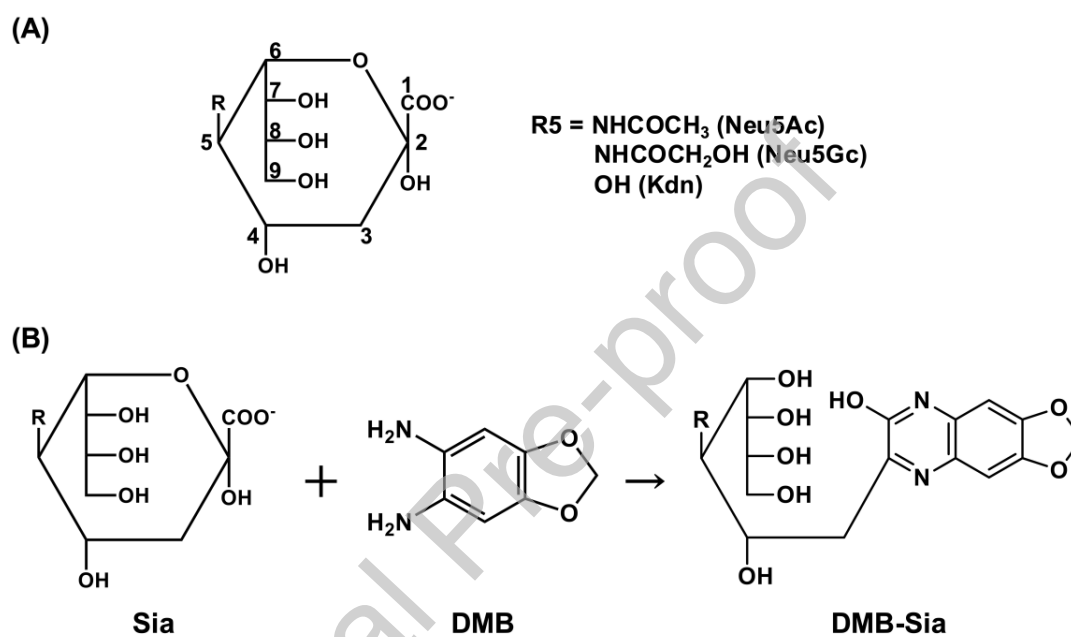


Fig. 1. Structures of sialic acids. (A) Structures of three major sialic acids species. R can be NHCOCH₃ (Neu5Ac), NHCOCH₂OH (Neu5Gc), or OH (Kdn). (B) The scheme of derivatization of sialic acids with DMB.

Fig. 1. Structures of sialic acids. (A) Structures of three major sialic acids species. R can be NHCOCH₃ (Neu5Ac), NHCOCH₂OH (Neu5Gc), or OH (Kdn). (B) The scheme of derivatization of sialic acids with DMB.

Fig. 2 (Omoto et al.)

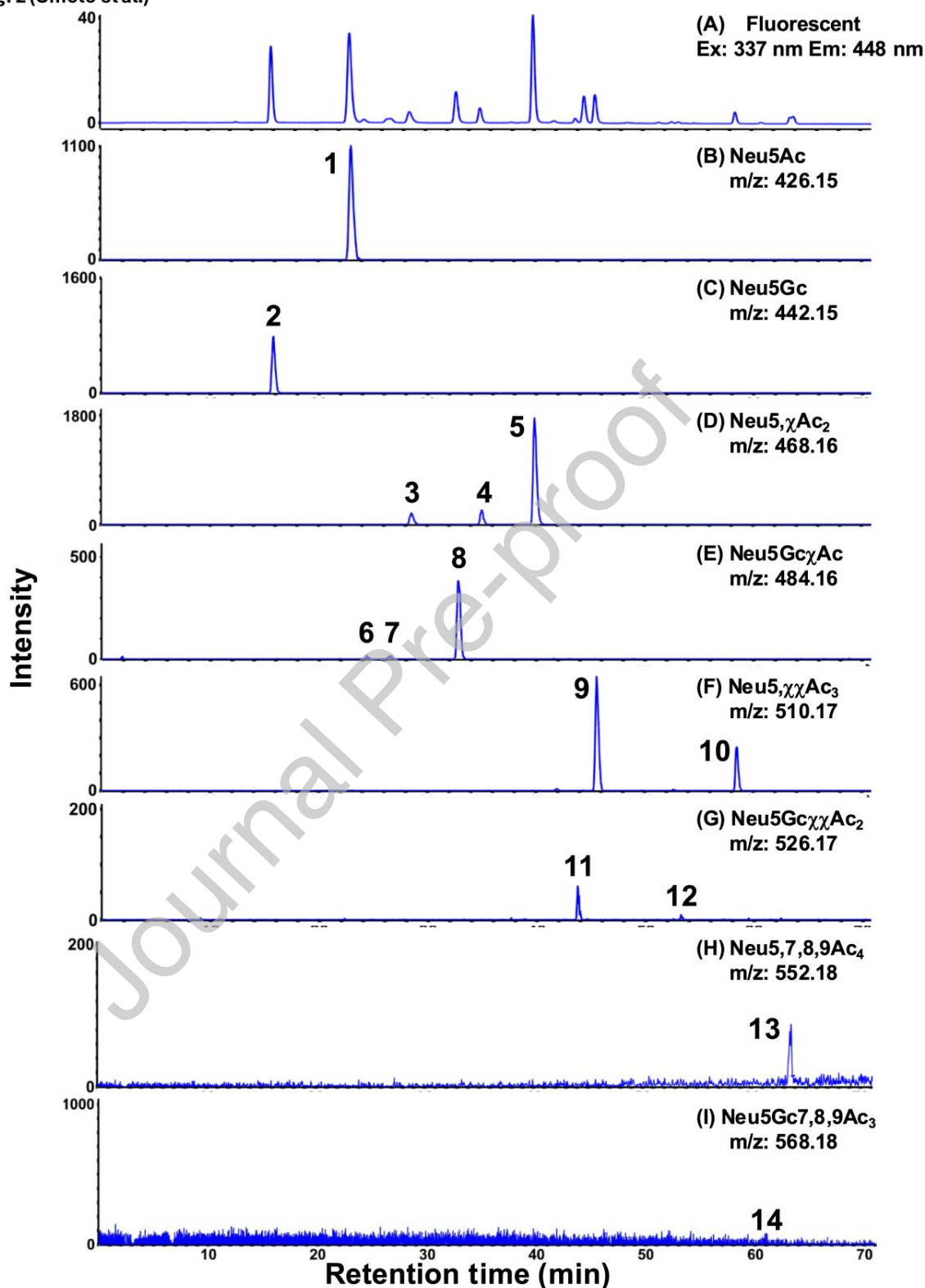


Fig. 2. LC-Fluorescence Detection-MS analysis for DMB-derivatized sialic acids in BSM. (A) Fluorescence (Ex/Em: 373/448 nm). (B) XIC at m/z 426.151 (Neu5Ac). (C) XIC at m/z 442.146 (Neu5Gc). (D) XIC at m/z 468.161 (Neu5, γ Ac). (E) XIC at m/z 484.156 (Neu5Gc γ Ac). (F) XIC at m/z 510.172 (Neu5, $\gamma\gamma$ Ac₃). (G) XIC at m/z 526.167 (Neu5Gc $\gamma\gamma$ Ac₂). (H) XIC at m/z 552.182 (Neu5,7,8,9Ac₄). (I) XIC at m/z 568.178 (Neu5Gc7,8,9Ac₃).

Fig. 2. LC-MS chromatograms and mass spectra of DMB-derivatized sialic acids (14 types) in BSM. (A) Fluorescence detection (Ex/Em: 373/448 nm). (B) XIC at m/z 426.151 (Neu5Ac). (C) XIC at m/z 442.146 (Neu5Gc). (D) XIC at m/z 468.161 (Neu5, χ Ac). (E) XIC at m/z 484.156 (Neu5Gc χ Ac). (F) XIC at m/z 510.172 (Neu5, $\chi\chi$ Ac₃). (G) XIC at m/z 526.167 (NeuGc $\chi\chi$ Ac₂). (H) XIC at m/z 552.182 (Neu5,7,8,9Ac₄). (I) XIC at m/z 568.178 (Neu5Gc7,8,9Ac₃).

Fig. 3 (Omoto et al.)

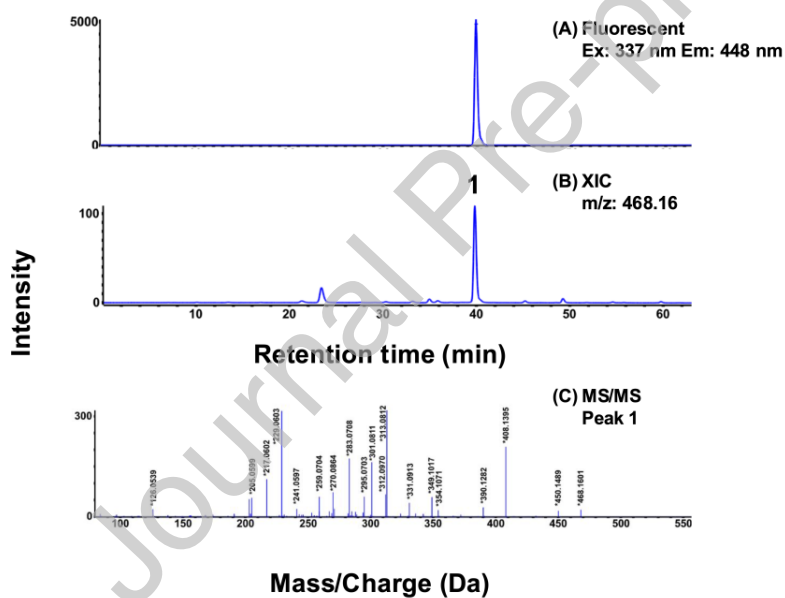


Fig. 3. LC-MS/MS chromatograms and mass spectra of DMB-derivatized standard Neu4,5Ac₂. (A) Fluorescence detection (Ex/Em: 373/448 nm). (B) XIC at m/z 468.16. (C) MS/MS fragmentation spectrum of peak 1.

Fig. 4 (Omoto et al.)

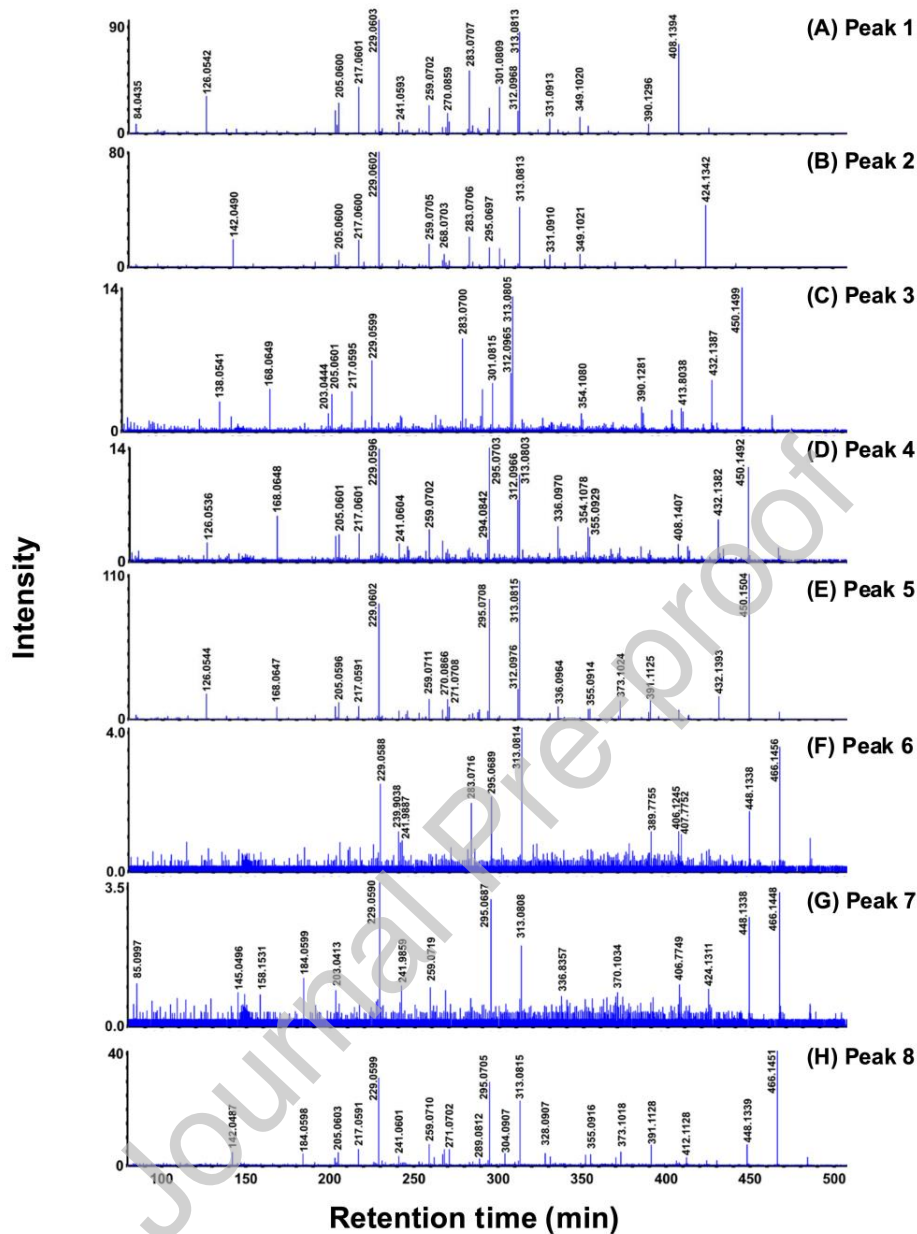


Fig. 4. LC-MS/MS fragmentation spectrum of Neu5Ac, Neu5Gc and mono-*O*-acetylated sialic acids (8 types) in BSM. (A) MS/MS spectrum of Peak 1 (Neu5Ac). (B) MS/MS spectrum of Peak 2 (Neu5Gc). (C) MS/MS spectrum of Peak 3, (D) Peak 4, and (E) Peak 5 (Neu5,cAc₂). (F) MS/MS spectrum of Peak 6, (G) Peak 7, and (H) Peak 8 (Neu5GccAc).

Fig. 5 (Omoto et al.)

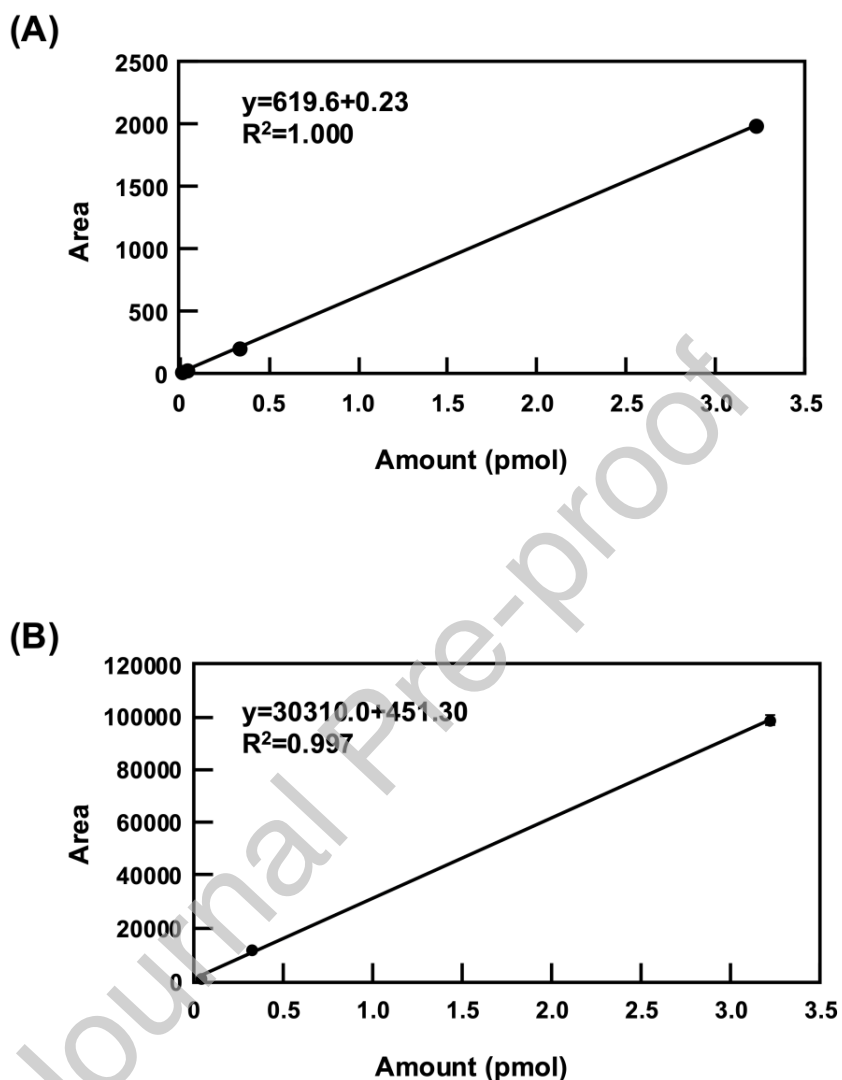


Fig. 5. Sensitivity comparison of fluorescence detection and sMRM^{HR} for DMB-derivatized standard Neu5Ac. Calibration curves were generated using triplicate measurements of 10-fold serial dilutions ranging from 3.2 pmol to 3.2 amol of standard Neu5Ac. Peak areas were

quantified for both detection methods. (A) Fluorescence detection (Ex/Em: 373/448 nm) with a detection limit of 320 amol. (B) XIC of sMRM^{HR} chromatogram with a detection limit of 320 fmol.

Journal Pre-proof

Fig. 6 (Omoto et al.)

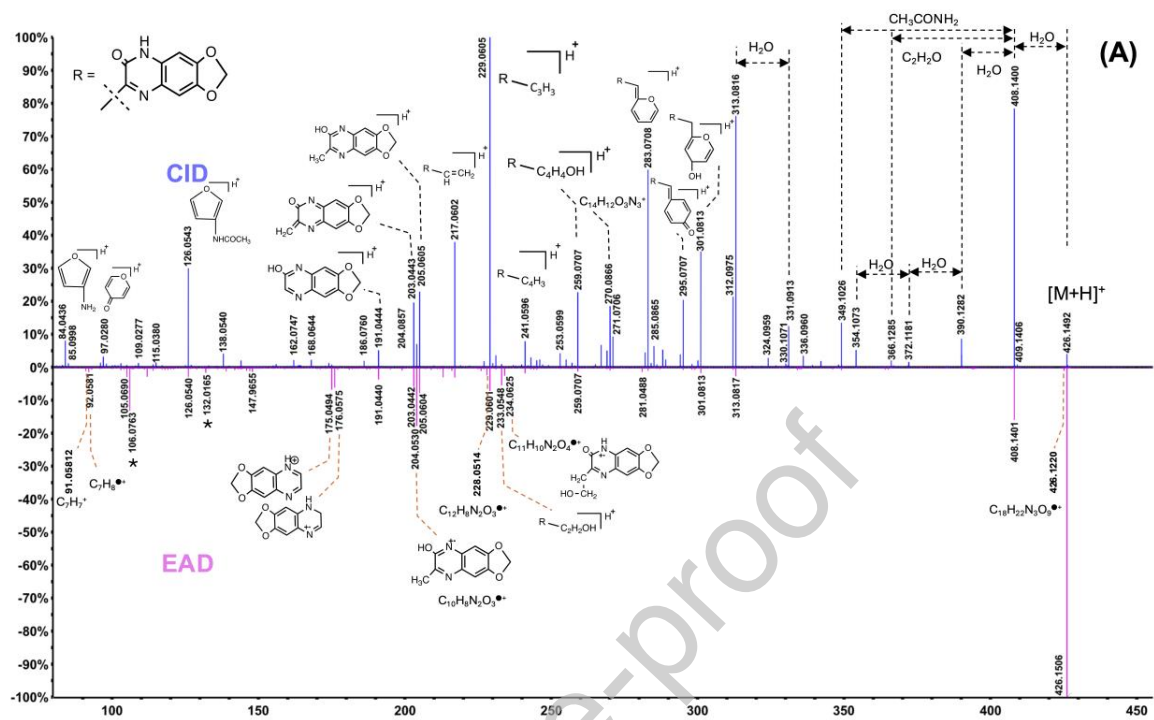


Fig. 6 (Omoto et al.)

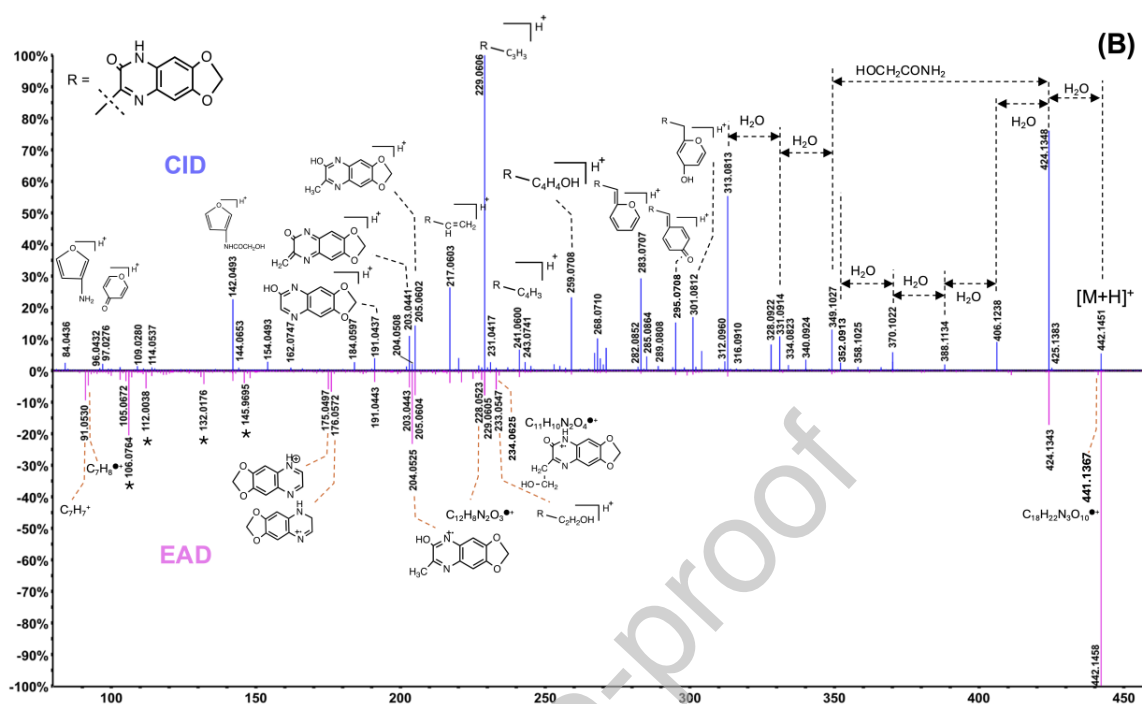


Fig. 6 (Omoto et al.)

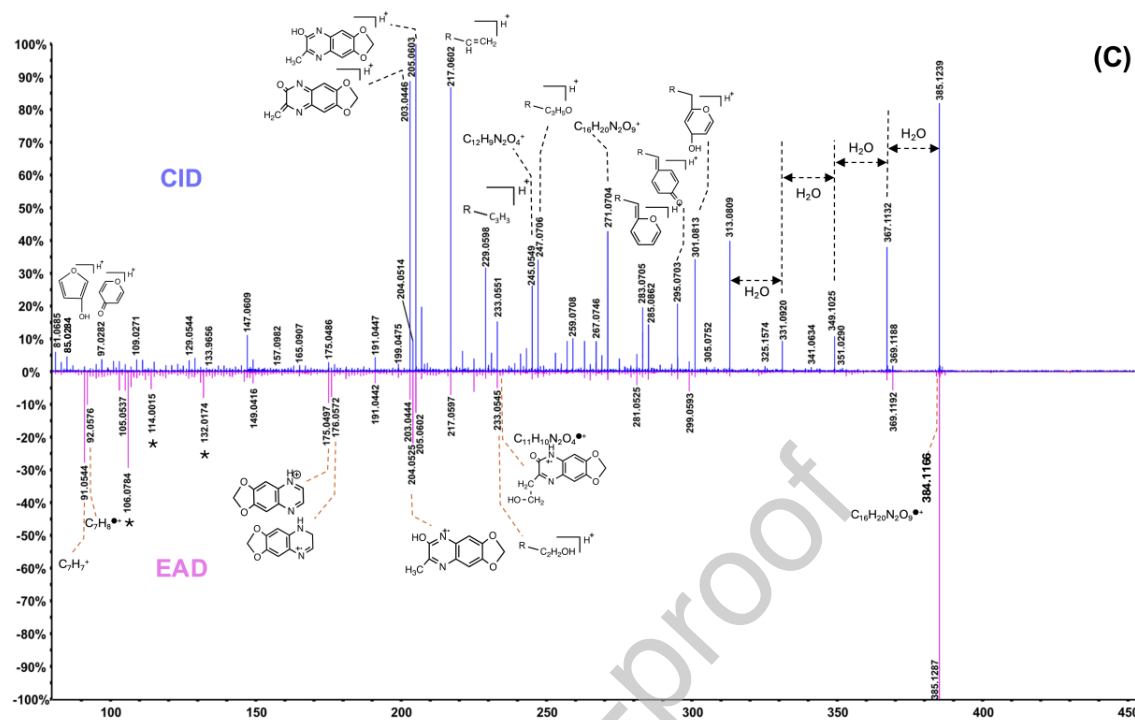


Fig. 6. Comparison with EAD fragmentation with CID of DMB-derivatized standard Sias. The fragmentation patterns of CID (*upper*) and EAD spectra (*lower*) from 1 ng of standard Neu5Ac (A), Neu5Gc (B), and Kdn (C). Each spectrum was shown at CAD30 for CID and KE of 16 eV for EAD fragmentation.

Fig. 6. Comparison with EAD fragmentation with CID of DMB-derivatized standard Sias. The fragmentation patterns of CID (*upper*) and EAD spectra (*lower*) from 1 ng of standard Neu5Ac (A), Neu5Gc (B), and Kdn (C). Each spectrum was shown at CAD30 for CID and KE of 16 eV for EAD fragmentation.

Supplementary figure legends

Fig. S1. LC-MS chromatograms and mass spectra of DMB-derivatized Neu5Ac, Neu5Gc, Kdn, and Neu5,9Ac₂ in reference standards (6 types). (A) Fluorescence detection (Ex/Em: 373/448 nm). (B) XIC at m/z 426.151 (Neu5Ac). (C) XIC at m/z 442.146 (Neu5Gc). (D) XIC at m/z 385.124 (Kdn). (E) XIC at m/z 468.161 (Neu5,γAc₂).

Fig. S2. LC-MS/MS fragmentation spectrum of standard Neu5Ac, Neu5Gc, Kdn, and mono-*O*-acetylated sialic acids. (A) MS/MS spectrum of Peak 1 (Neu5Ac). (B) MS/MS spectrum of Peak 2 (Neu5Gc). (C) MS/MS spectrum of Peak 3 (Kdn). (D) MS/MS spectrum of Peak 4 (Neu5,7Ac₂). (E) MS/MS spectrum of Peak 5 (Neu5,8Ac₂). (F) MS/MS spectrum of Peak 6 (Neu5,9Ac₂).

Fig. S3. LC-MS/MS fragmentation spectrum of di-, tri- and tetra-*O*-acetylated sialic acids in BSM. (a) MS/MS spectrum of Peak 9 and (b) Peak 10 (Neu5,γγAc₃). (c) MS/MS spectrum of Peak 11 and (d) Peak 12 (Neu5GcγγAc₂). (e) MS/MS spectrum of Peak 13 (Neu5,7,8,9Ac₄). (f) MS/MS spectrum of Peak 14 (Neu5Gc7,8,9Ac₃).

Fig. S4. LC-MS/MS chromatograms and mass spectra of DMB-derivatized Neu5Gc7,8,9Ac₃ in 50 ng BSM. (A) Fluorescence detection (Ex/Em: 373/448 nm). (B) XIC at m/z 568.18. (C) MS/MS spectrum of peak 14.

Table 1
Relative retention times and observed characteristic ion set for sialic acid species in BSM analyzed by LC-MS/MS CID at CAD30

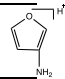
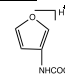
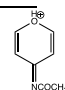
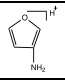

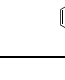
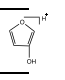
Peak No.	Sialic acid	RRT (min)	[M+H] ⁺ m/z	[M+H-18] ⁺ m/z	Observed characteristic ion set m/z
1	Neu5Ac	1.00	426.1 5	408.15	229, 313, 283, 301, 217, 126 , 205
2	Neu5Gc	0.69	442.1 5	424.15	229, 313, 283, 142 , 217, 259, 295
3	Neu5,7Ac ₂	1.24	468.1 6	450.16	313, 283, 229, 312, 301, 295, 168
4	Neu5,8Ac ₂	1.52	468.1 6	450.16	295, 229, 313, 312, 168 , 203, 354, 355
5	Neu5,9Ac ₂	1.73	468.1 6	450.16	313, 295, 229, 312, 126 , 270, 355
6	Neu5Gc7Ac	1.06	484.1 6	466.16	313, 229, 295, 283, 241
7	Neu5Gc8Ac	1.16	484.1 6	466.16	229, 295, 313, 184 , 259, 203
8	Neu5Gc9Ac	1.43	484.1 6	466.16	229, 295, 313, 259, 217, 142 , 184
9	Neu5, $\chi\chi$ Ac ₃₋₁	1.98	510.1 7	492.17	295, 313, 229, 312, 267, 354, 355
10	Neu5, $\chi\chi$ Ac ₃₋₂	2.54	510.1 7	492.17	295, 229, 336, 313, 312, 354, 168
11	Neu5Gc $\chi\chi$ Ac ₂₋₁	1.90	526.1 7	508.17	295, 313, 229, 355, 370, 286
12	Neu5Gc $\chi\chi$ Ac ₂₋₂	2.32	526.1 7	508.17	286, 229, 295, 259, 313
13	Neu5,7,8,9Ac ₄	2.77	552.1 8	534.18	295, 355, 312, 168
14	Neu5Gc7,8,9Ac ₃	2.24	568.1 8	550.18	295, 229, 312

* Relative retention time (RRT) is a relative value indicating the retention time of each sialic acid species observed in BSM in relation to that of Neu5Ac.

The ions colored red are specific ions that reflect the differences in the substituents of carbon-5, which were identified as diagnostic ions in this study (Table 2).

Table 2
Predicted structures and sum formulas of C5-specific diagnostic ions in MS/MS fragments of three major sialic acid species

*Relative retention time (RRT) is a relative value indicating the retention time of each sialic acid species in

Peak No.	Sialic acid	RR T (min)	[M+H] ⁺ m/z	[M+H-18] ⁺ m/z	Observed characteristic ion set m/z	C5-specific diagnostic ions		
						m/z	Molecular formula	Structure
1	Neu5Ac	1.00	426.15	408.15	229, 313, 283, 217, 301, 126, 205	84.044 39	C4H6NO +	
						126.05 495	C6H8NO 2+	
						138.05 495	C7H8N1 O2+	
						168.06 552	C8H10N O3+	n.p.
2	Neu5Gc	0.68	442.15	424.15	229, 313, 283, 217, 259, 142, 301	84.044 39	C4H6NO +	
						142.04 987	C6H8NO 3+	
						154.04 987	C7H8N1 O3+	
						184.06 043	C8H10N O4+	n.p.
3	Kdn	0.54	385.12	367.12	205, 203, 217, 271, 313, 301, 247	85.028 41	C4H5O2 +	
						127.03 897	C6H7O3 +	n.p.
						129.05 462	C6H9O3 +	n.p.

relation to that of Neu5Ac.

n.p., not predicted. The ions colored red are specific ions that reflect the differences in the substituents of carbon-5, which we have distinguished as diagnostic ions in this study.

Declaration of interests

The authors declare that they have no known competing financial interests or personal relationships that could have appeared to influence the work reported in this paper.